Influence of the Sequestration Effect of CTAB on the Biofunctionalization of Gold Nanorods

Henryk J Łaszewski, Bruno Palpant, Malcolm Buckle, Claude Nogues

ACS APPLIED BIO MATERIALS

www.acsabm.org Article

Influence of the Sequestration Effect of CTAB on the Biofunctionalization of Gold Nanorods

Henryk J. Łaszewski, Bruno Palpant, Malcolm Buckle, and Claude Nogues*

Cite This: https://doi.org/10.1021/acsabm.0c01522 Read Online

ACCESS | Metrics & More | Article Recommendations | Supporting Information

ABSTRACT: Gold nanorods (GNRs) can be functionalized with multiple biomolecules allowing efficient cell targeting and delivery into specific cells. However, various issues have to be addressed prior to any clinical applications. They involve controlled biofunctionalization to be able to deliver a known dose of drug by immobilizing a known number of active molecules to GNRs while protecting their surface from degradation. The most widely used synthesis method of GNRs is seed-mediated growth. It requires the use of cetyltrimethylammonium bromide (CTAB) that acts as a strong capping agent stabilizing the colloidal solution. The problem is that not only is CTAB cytotoxic to most cells but it also induces the sequestration of biomolecules in solution during the functionalization steps of GNRs. The presence of CTAB therefore makes it difficult to control the immobilization of biomolecules to GNRs while removing CTAB from the colloidal solution, leading to the aggregation of GNRs. The sequestration effect of ssDNA in solution by CTAB was studied in detail as a function of the CTAB concentration and the nature of the solution (water or buffer) using Forster resonance energy transfer as a detection tool. The conditions in which DNA sequestration did and did not occur could be clearly defined. Using gel electrophoresis, we could demonstrate how strongly the ssDNA sequestration effect in solution impacts the GNR surface biofunctionalization.

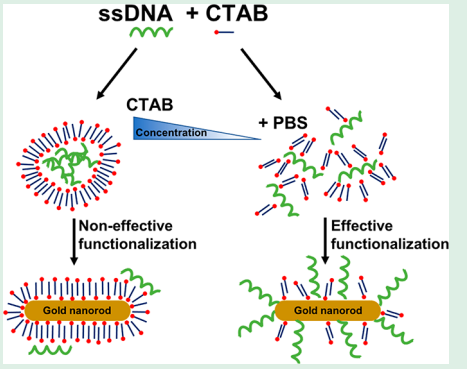

KEYWORDS: *gold nanorods, CTAB, functionalization, DNA, FRET*

INTRODUCTION

Gold nanorods (GNRs) are plasmonic nanoparticles with attractive optical properties for biomedical applications including biosensing, biomedical imaging, drug delivery, and cancer diagnosis and therapy.[1−5] More specifically, drug delivery using GNRs as a cargo to specific organs or cells can significantly improve the efficiency of treatments while minimizing the side effects. For cancer, most dysfunctions originate from the expression of (i) mutated genes or (ii) dysregulated genes that overexpress proteins in cells.[6] Deactivating a defective gene using an antisense oligonucleotide (ASO) (DNA, RNA, or a chemical analogue) or a small interfering RNA (siRNA) can therefore revolutionize the treatment of cancer.[7−9] Even though the antisense strategy was discovered over 20 years ago and despite intense pharmaceutical research, only a few drugs have been approved by the US Food and Drug Administration (FDA), mainly due to different types of challenges including toxicity, tissue penetration, delivery at a specific tissue, and type of cells.

GNRs can be functionalized with multiple biomolecules allowing efficient cell targeting and delivery into specific cells.[10] In addition, GNRs potentially exhibit low cytotoxicity when they are carefully biofunctionalized and are readily internalized by cancer cells because of their high membrane permeability.[11] However, different issues have to be addressed before any clinical application, including controlled biofunctionalization to be able to deliver a known dose of drug, bio distribution of the drug-GNRs, and stability under biological environment as well as the fate of GNRs after their administration to patients. One of the first challenges is therefore to immobilize a known quantity of a specific drug to GNRs while protecting their surface from degradation.

The most widely used synthesis method of GNRs is seed-mediated growth because of the ease of controlling the GNRs aspect ratio and its high yield.[12] This method requires the use of cetyltrimethylammonium bromide (CTAB) as a strong capping bilayer surfactant.[13] CTAB-coated GNRs are positively charged and the electrostatic repulsion in aqueous solution stabilizes GNRs. In buffered solution or in complex media (serum or cell culture media for example) the CTAB-stabilized GNRs aggregate extremely quickly due to the reduction of repulsive interactions between GNRs, unless a large excess of CTAB is maintained in solution (between 1 and 5 mM).[14] The problem is that CTAB exhibits cytotoxicity to most cells when in solution or adsorbed on the GNRs

Received: November 22, 2020
Accepted: May 12, 2021

surface.[15] It is thus of primary importance to remove CTAB from the solution and replace it on the GNRs' surface prior to any biomedical applications.

The replacement of CTAB is generally performed by GNRs surface modification methods that include ligand exchange, layer-by-layer (LBL), or surface coating by a silica layer[16] or a polymer.[17,18] The ligand exchange consists in replacing CTAB by phosphatidylcholine (PC), lipids, or thiolated molecules.[19−23] Indeed, thiolated molecules can form stable and dense monolayers on gold with a strong chemical S−Au bond, resulting in an efficient protecting surface layer that also reduces cytotoxicity. In order to both replace CTAB from the GNRs surface and to protect GNRs against aggregation, the ligand exchange has to be performed with a large excess of thiolated molecules in solution. This is possible with molecules such as, for example, thiol-terminated poly(ethylene glycol) (PEG-SH)[22] or 11-mercaptoundecanoic acid.[24]

Molecules with a carboxylic acid group at the extremity opposite the thiol group can be used to immobilize biomolecules via the formation of an amide bond with a primary amine present in the ligand. This biofunctionalization method first necessitates activation of the carboxylic group, rinsing off any excess of the activator molecules from the colloidal solution, and then incubation of the GNRs with the ligand. Although this biofunctionalization method is efficient, it is also time-consuming. The cycles of centrifugation and redispersion of the sample lead to a significant decrease of the GNRs concentration in solution. In addition, the ligand surface density and its distribution on each GNRs surface is extremely difficult to control.

One effective method is the direct immobilization of thiolated DNA (single, ss or double, ds strands) to the GNRs surface but two obstacles must be overcome. First, the concentration range of the thiolated DNA stock solution does not exceed a few hundred micromolar (μM). Second, either ssDNA or dsDNA interacts strongly with the CTAB present in the colloidal solution preventing DNA from being homogeneously distributed in the solution. The sequestration effect of CTAB on DNA diluted in water and in saline buffer is known and well described.[25] It depends on different parameters such as the CTAB concentration, the presence of salt in solution and finally, on the nature of the DNA (double- versus single-strand DNA, and length). The critical micellar concentration (CMC) of CTAB in pure water is 0.92 to 1 mM.[26] Therefore, when adding ssDNA to a GNR solution with 5 mM CTAB, most of the ssDNA interacts electrostatically with the surface of the CTAB micelles and/or with the CTAB double layer at the surface of GNRs.[27] Therefore, the sequestration effect of CTAB must strongly influence the immobilization of thiolated-ssDNA on the GNRs surface and strongly impede controlled DNA immobilization through the S−Au bond on the GNRs surface.

In this work, we focus on understanding the influence of the interactions between ssDNA and CTAB on the functionalization of GNRs. The goal is to find conditions where ssDNA sequestration by CTAB is minimized so that GNRs surface functionalization can be optimized and controlled. First, to study in detail the sequestration of ssDNA in solution we chose to use FRET (Forster Resonance Energy Transfer) as a detection tool. Two non-complementary ssDNA sequences labeled with a couple of fluorophores for FRET experiments were introduced to increasing concentrations of CTAB diluted in an aqueous solution or saline buffer solution (PBS). FRET would be detected in situations where both non-complementary strands are in close proximity due to the sequestration effect of CTAB, while no FRET should be detected when both DNA strands are homogeneously distributed in solution. Finally, to illustrate how strongly the ssDNA sequestration by CTAB impacts on the GNR surface biofunctionalization, GNRs were incubated with thiolated-ssDNA in conditions where either sequestration was clearly identified or, on the contrary, where no sequestration of DNA was detected. Gel electrophoresis monitoring the emission intensity of the labeled thiolated-ssDNA bound to the GNRs surface was used to estimate the ssDNA immobilization efficiency.

MATERIALS AND METHODS

Agarose, phosphate buffer saline (PBS), cetyltrimethylammonium bromide (CTAB), chloroauric acid, sodium borohydrate, silver nitrate, L-ascorbic acid and tris-borate-EDTA buffer (TBE) were purchased from Sigma-Aldrich.

Labeled DNA sequences were purchased from Sigma-Aldrich: $^{5'}$CCA TCT GTC ACT CGG ATC CGC CAT CTT GCG ACT CG$^{3'}$-Cy3 (D1-Cy3); Cy5-$^{5'}$CGA GTC GCA AGA TGG CGG ATC CGA GTG ACA GAT GG$^{3'}$ (D1-Cy5); Cy5-$^{5'}$GCT CAG CGT TCT ACC GTA TAT TCT CAC TGT CTA CC$^{3'}$ (D2-Cy5). SH-D1-Cy3: SH-C_6H_{12}-T5-D1-Cy3.

D1-Cy3 and D1-Cy5 are complementary strands while D1-Cy3 and D2-Cy5 are non-complementary strands. SH-D1-Cy3 is the sequence used to functionalize GNRs.

GNRs Synthesis. The initial step for synthesis of GNRs involved seed formation, in which small nanoparticles were formed. A solution of 900 μL of ice-cold NaBH4 at 0.01 M was injected into a mixture containing 9.8 mL of 0.1 M CTAB and 250 μL of 0.01 M $HAuCl_4$. After 2 min of vigorous stirring the seed solution was directly added to a growth solution preprepared by diluting 0.1 M of CTAB and 2.5 mL of 0.01 M $HAuCl_4$ to a final volume of 50 mL. After 10 min of incubation, 375 μL of 0.1 M L-ascorbic acid were injected for gold(III) reduction to gold(I). Gentle mixing caused the pale-orange solution to shift to colorless indicating that the reaction had occurred. Then, 400 μL of 5 mM $AgNO_3$ was added to allow the growth of nanorods. The solution with growing nanoparticles was incubated for 2 h. In order to remove the excess of chemicals from the growth solution and to decrease the concentration of CTAB from 93 mM to 5 mM, the growth solution was rinsed twice. The rinsing process consisted of centrifugation, removal of the supernatant, and redispersion of the GNRs in pure water. To characterize the GNRs colloidal solution, the absorption spectrum was measured and the GNRs were visualized using transmission electron microscopy (TEM) (Figure S1 of the Supporting Information, SI). The concentration of GNRs in solution was 0.18 nM, an estimation based on absorption spectroscopy using the method described by Orendorff and Murphy.[28]

FRET Measurements. FRET experiments were performed on a fluorescence spectrophotometer Eclipse CARRY. The two labeled ssDNA strands were mixed by adding 10 nM of each oligonucleotide in solutions of different CTAB concentrations: either the oligonucleotides were premixed and then added to the CTAB solutions (mix DNA), or the two oligonucleotides were added one after the other directly into the CTAB solutions (step DNA). For FRET experiments the excitation wavelength was fixed at 530 nm to excite Cy3.

GNRs Functionalization. 850 μL of water were mixed with 150 μL of GNRs stock solution (0.18 nM of GNRs and 5 mM CTAB) resulting in a colloidal solution in 0.75 mM CTAB. Alternatively, 700 μL of 1× PBS, 5 mM CTAB solution were mixed with 150 μL of 2× PBS, 5 mM CTAB, and GNRs (0.18 nM diluted in 5 mM CTAB in water), resulting in a colloidal solution in 1× PBS, 5 mM CTAB. The oligonucleotides (stock solution at 100 μM) were added to the freshly prepared GNRs solution so the final ssDNA concentration would be 20, 150, 300, and 500 nM, incubated for 4 h. Then 20 μL of Tween20

https://doi.org/10.1021/acsabm.0c01522
ACS Appl. Bio Mater. XXXX, XXX, XXX−XXX

were added and incubated for 30 min. Subsequently, samples were centrifuged for 30 min at 8000 rcf and GNRs were rinsed with a 2% Tween20 aqueous solution. This step was repeated one more time to reduce the CTAB concentration to approximately 0.02 mM. A third centrifugation step was then applied, and the redispersion in this last step was performed with pure water. In all the rinsing steps, 98% of the total volume was exchanged.

Gel Electrophoresis. The agarose gels were prepared by mixing 0.8% in mass of agarose powder in 1× TBE. Nine μL of the sample solution was loaded into the wells and run for 40 min at 50 V in 1× TBE. Subsequently, the gels were characterized using a Typhoon scanner to collect absorption and fluorescence images.

RESULTS AND DISCUSSION

To characterize in detail the sequestration of ssDNA by CTAB in water and in PBS, two non-complementary ssDNA labeled respectively with Cy3 and Cy5 were mixed in water. The mixed ssDNA was diluted either in water (No CTAB) or in 1 mM CTAB. The fluorescence emission spectra collected between 550 and 800 nm were recorded upon excitation of Cy3 at 530 nm (Figure 1).

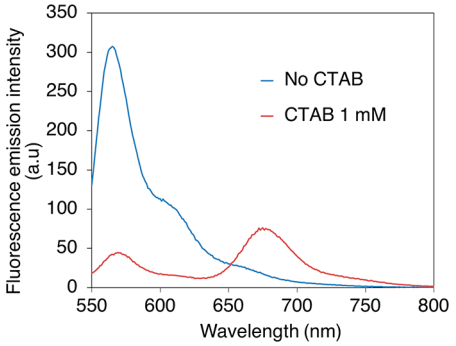

Figure 1. Fluorescence emission intensity of two non-complementary ssDNA labeled with Cy3 and Cy5 (D1-Cy3 and D2-Cy5) premixed in pure water, then diluted in water (No CTAB) or in 1 mM CTAB. The excitation wavelength is 530 nm (excitation wavelength of Cy3).

In water, the spectrum corresponds to that of pure Cy3 with a maximum peak emission at 563 nm (Figure S2). Indeed, the two ssDNA strands are noncomplementary, therefore, no FRET was to be expected. Surprisingly, in 1 mM CTAB, the intensity of the maximum emission peak of Cy3 decreased significantly compared to the maximum intensity measured in pure water and a peak at 660 nm corresponding to the emission of Cy5 could clearly be detected. The emission of Cy5 upon excitation of Cy3 reveals that the resonance energy is transferred from the donor (Cy3) to the acceptor (Cy5). Although the strong decrease of the Cy3 emission intensity upon addition in the CTAB solution may be partially due to the quenching effect of CTAB (Figure S2), the concomitant growing emission peak of Cy5 implies that both non-complementary ssDNA were maintained close enough to allow FRET when the premixed ssDNA solution was introduced in the 1 mM CTAB solution. It can be noticed that Cy5 emission is also partially quenched by CTAB (Figure S3).

In order to account for the CTAB quenching effect on the emission intensity of both Cy3 and Cy5 (Figures S2 and S3), we calculated the FRET efficiency for each CTAB concentration both in water and in PBS according to eq 1.

$$E_{FRET} = 1 - I_{DA}/I_D \quad (1)$$

where I_{DA} and I_D are the integrated peak intensities of the donor (between 550 and 800 nm) in the presence (I_{DA}) and in the absence (I_D) of the acceptor, respectively.

The calculated FRET efficiency of the premixed ssDNA solution diluted in pure water and in CTAB solutions at different concentrations ranging from 0.001 mM to 10 mM is presented in Figure 2. The premixed ssDNA is composed of

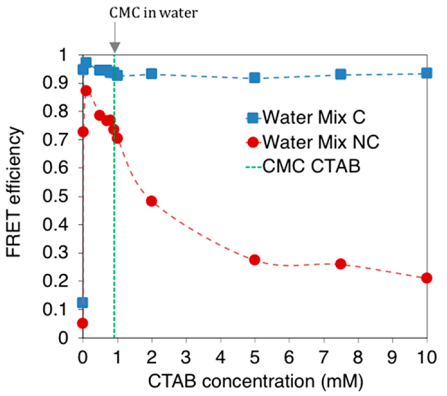

Figure 2. FRET efficiency of a premixed non-complementary (NC) or complementary (C) ssDNA as a function of the CTAB concentration in aqueous solution. The CMC of CTAB (0.92 mM)[26] is indicated as a vertical line. Each point corresponds to the FRET efficiency averaged over 3 independent sample measurements. The maximum standard deviation is 7×10^{-4}.

the two non-complementary DNAs (NC) labeled with Cy3 and Cy5 respectively as shown in Figure 1. As a control two complementary ssDNA (C) labeled with Cy3 and Cy5 were premixed before their dilution in water with increasing concentrations of CTAB.

The calculation of the FRET efficiency confirmed that at 1 mM CTAB (CMC), FRET was detected for non-complementary ssDNA with an efficiency of 70% while 4% FRET efficiency was detected in pure water (in the absence of CTAB). The FRET efficiency in water should have been null since no FRET is expected for non-complementary DNA. The weak detected emission intensity from Cy5 is due to its direct excitation upon excitation of Cy3 corresponding to 4% of the total measured FRET efficiency (Figures S4 and S5). Indeed, a clear emission peak at 660 nm, corresponding to the emission wavelength of Cy5, is detected when a pure D2-Cy5 solution is excited at the excitation wavelength of Cy3 (Figure S4). In Figure S5 we can clearly distinguish a shoulder at 660 nm, corresponding to the emission of D2-Cy5 in the presence of D1-Cy3, upon excitation at 530 nm (the excitation wavelength of Cy3).

For CTAB concentrations lower than the CMC, the FRET efficiency for two non-complementary strands increased rapidly to 87% at 0.1 mM and then decreased to 70% at 1 mM. As the concentration of CTAB increased above the CMC, the FRET efficiency decreased gradually to reach approximately 25% between 5 to 10 mM. When the two ssDNA were complementary, the FRET efficiency increased from 12% in pure water to 95% as soon as CTAB was present in solution (from 0.001 mM of CTAB) and remained constant regardless of the CTAB concentration (Figure 2).

In PBS (Figure S6), an identical behavior was observed. The sequestration effect of DNA from a premixed ssDNA solution diluted in a solution containing CTAB did not depend on the

https://doi.org/10.1021/acsabm.0c01522
ACS Appl. Bio Mater. XXXX, XXX, XXX−XXX

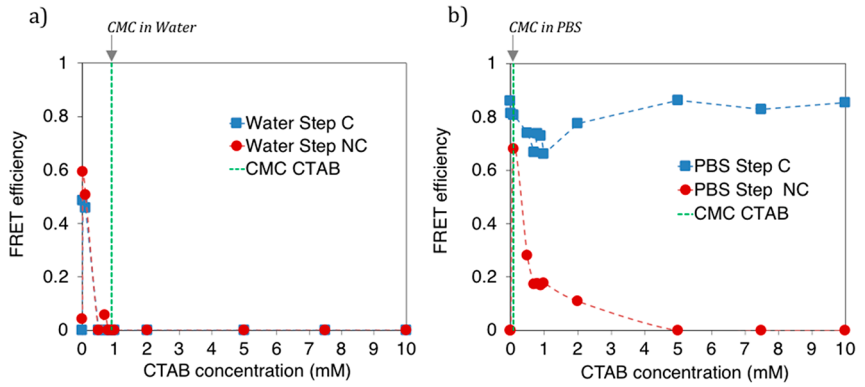

Figure 3. FRET efficiency of two non-complementary (NC) and complementary (C) ssDNA introduced step-by-step in (a) water or (b) PBS without CTAB or with CTAB at increasing concentration ranging from 0.01 to 10 mM. The CMC of CTAB in water (0.92 mM)[26] and in PBS (0.074 mM)[30] are indicated by a vertical dotted line. Each point corresponds to the FRET efficiency calculation averaged over 3 independent sample measurements. The maximum standard deviation is 9×10^{-4}.

presence of salt. The sequestration effect was more substantial for CTAB concentrations lower than the CMC as we observed strong FRET for non-complementary ssDNA both in water and in PBS. Above the CMC, although the FRET efficiency decreased significantly for non-complementary ssDNA the sequestration effect was still large.

Since the sequestration of ssDNA in solution is strongly influenced by the concentration of CTAB, we suspect that (i) for CTAB concentrations lower than the CMC, DNA is immediately sequestered. CTAB molecules interact with the ssDNA backbone and fluorophore forming small compartments that maintain DNA in very close proximity (high FRET for non-complementary ssDNA); (ii) for CTAB above the CMC, DNA interacts with the surface of the positively charged vesicles as shown using imagery methods.[29] The density of DNA on the vesicle surface is such that FRET could still be detected between two labeled non-complementary ssDNA. For CTAB around the CMC, both free CTAB molecules and vesicles are present in solution, contributing to ssDNA sequestration.

To confront this hypothesis, we tested the influence of successive addition of both ssDNA in pure water or in PBS with and without CTAB on the FRET efficiency (Figure 3).

The sequential addition of ssDNA in water did not lead to FRET for non-complementary and for complementary ssDNA at CTAB concentration higher than the CMC. Under the CMC, the FRET efficiency increased from ∼0% in pure water to 60% at 0.01 mM CTAB. Then, the FRET efficiency decreased rapidly down to ∼0% as the CTAB concentration was increased gradually up to the CMC. As discussed with the mix-ssDNA, the introduction of ssDNA to the aqueous CTAB solution induces its immediate sequestration due to the electrostatic interactions between free CTAB molecules and the ssDNA phosphate backbone. The addition of a second ssDNA in a solution containing a low concentration of CTAB (between 0.01 and 0.1 mM) apparently leads to its incorporation in the compartment where the first ssDNA was sequestered. For CTAB concentrations higher than 0.1 mM, it appears that the interaction between free CTAB and the phosphate backbone of ssDNA is sufficient to keep both ssDNA strand separated. In PBS, the situation is very different.

In pure PBS, the FRET efficiency reached 80% for complementary strands while no FRET was detected for non-complementary strands. Then the FRET efficiency for complementary strands in PBS and at CTAB concentration ranging from 0.1 to 1 mM decreased to approximately 70% and then increased back to 80% from 2 mM CTAB. For non-complementary ssDNA, the FRET efficiency decreased rapidly from approximately 70% at 0.1 mM CTAB down to 17% at 1 mM CTAB concentration and finally to 0% above ∼5 mM CTAB.

Therefore, below 0.1 mM CTAB concentration ssDNA were sequestered together despite the sequential addition of both ssDNA strands leading to a strong FRET detection. For CTAB concentrations above 0.1 mM in PBS, we observed a high FRET efficiency for the two complementary ssDNA and a much lower FRET efficiency for the non-complementary ssDNA. Above 5 mM CTAB and in the presence of PBS, no FRET was observed for the non-complementary stands while the FRET efficiency for the two complementary strands was at its maximum.

In water, ssDNA polyelectrolyte forms a complex with CTAB molecules at concentrations under the CMC.[31] Above the CMC, CTAB starts to form positively charged micelles in water so ssDNA interacts with and adsorbs to their surface allowing FRET between labeled non-complementary ssDNA.[29] The low FRET efficiency is due to the random interaction of the ssDNA to the micelle's surface placing both fluorophores in positions where FRET may occur or not. In PBS, the presence of counterions lowers the CTAB CMC since counterions decrease the electrostatic repulsion of the cationic CTAB surfactant, therefore promoting the formation of denser micelles.[32,33] The apparent charge of the CTAB micelles is therefore neutralized so ssDNA does not interact strongly with the micelle's surface. At high CTAB concentrations diluted in PBS (from 5 mM) the two complementary ssDNA strands can therefore hybridize (high FRET efficiency) while the two non-complementary ssDNA do not interact (no FRET). We conclude that in solution with CTAB concentrations higher than 5 mM diluted in PBS, no ssDNA sequestration effect could be detected.

To illustrate the importance of the ssDNA sequestration by CTAB on the GNR surface modification, GNRs were incubated with thiolated ssDNA-Cy3 (SH-D1-Cy3) in conditions where sequestration was clearly identified (0.75 mM CTAB in water) and where no sequestration of DNA could be detected (5 mM CTAB, 1x PBS).

https://doi.org/10.1021/acsabm.0c01522
ACS Appl. Bio Mater. XXXX, XXX, XXX−XXX

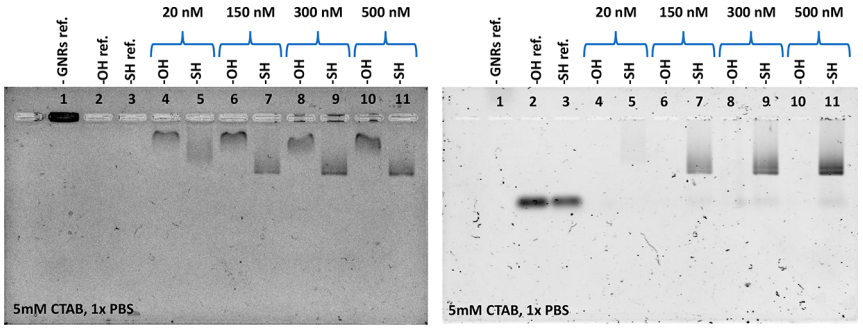

Figure 4. Agarose gel electrophoresis of GNRs incubated with different concentrations of D1-Cy3 and SH-D1-Cy3 in 5 mM CTAB in 1× PBS. (Left) contrast image; (right) fluorescence emission image. The samples were loaded as follow: 1- GNRs in 0.75 mM CTAB (reference); 2- and 3- D1-Cy3 and SH-D1-Cy3, respectively, at 20 nM (reference); lanes 4, 6, 8, and 10 are GNRs incubated with D1-Cy3 (−OH) at 20, 150, 300, and 500 nM, respectively; lanes 5, 7, 9, and 11 are GNRs incubated with SH-D1-Cy3 (-SH) at 20, 150, 300, and 500 nM, respectively.

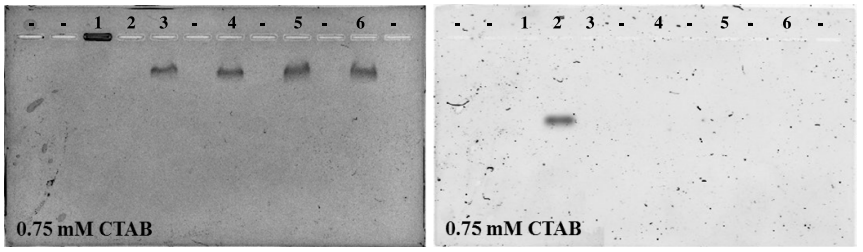

Figure 5. Agarose gel electrophoresis of GNRs incubated with different concentrations of SH-D1-Cy3 in 0.75 mM CTAB. (Left) Contrast image; (right) Fluorescence emission image. The samples were loaded as follow: 1-GNRs in 0.75 mM CTAB (reference), 2-SH-D1-Cy3 at 20 nM (reference), then lanes 3, 4, 5, and 6 are GNRs incubated with SH-D1-Cy3 at 20, 150, 300, and 500 mM, respectively.

The stability of the GNRs colloidal solution was verified by recording the absorption spectra of GNRs diluted in 0.75 mM CTAB and in 5 mM CTAB, 1x PBS (Figure S7). Both spectra were very similar and corresponded to typical spectra for stable colloidal solutions.[1] In addition, we observed no influence of the presence of the thiol modification of the ssDNA on the CTAB interaction (Figure S8).

The concentration of ssDNA in solution was 20, 150, 300, and 500 nM and GNRs were kept at 0.2 nM. The ssDNA to GNR ratio was chosen to obtain a high ssDNA surface coverage as described previously.[34] The detailed functionalization protocol is described in the Materials and Methods section. It is important to note that all samples were rinsed multiple times to remove all unbound ssDNA from the solution before sample characterization. To estimate the efficiency of the thiolated ssDNA surface immobilization on GNRs (SH-D1-Cy3), the non-thiolated Cy3 ssDNA (D1-Cy3) was also incubated with GNRs and loaded on the gel. To correlate the migration of GNRs with the migration of ssDNA, a direct contrast image of the gel and a fluorescence emission image of the same gel are presented, respectively, on the left and right panels of Figures 4 and 5.

On the left panel of the Figure 4, where only GNRs are visible, we observe that bare GNRs (lane 1) did not migrate in the gel despite the applied electrical potential. All GNRs that were incubated with D1-Cy3 or with SH-D1-Cy3 did clearly migrate. The distance of migration from the well depends strongly on the nature of DNA. Indeed, GNRs incubated with D1-Cy3 migrate at a much lower distance from the wells than GNRs incubated with SH-D1-Cy3. In addition, all samples prepared with D1-Cy3 migrate similarly while the SH-D1-Cy3 concentration used for the GNRs functionalization influenced the migration distance of GNRs.

On the fluorescence emission image (Figure 4, right panel), we do not observe the emission of fluorescence on lanes corresponding to GNRs incubated with D1-Cy3 (lanes 4, 6, 8, and 10). With GNRs incubated with SH-D1-Cy3 a clear migration pattern is detected. The migration pattern and contrast intensity depend strongly on the SH-D1-Cy3 concentration. The difference of migration distance and pattern of samples prepared with non-thiolated ssDNA and thiolated ssDNA demonstrates that the immobilization of ssDNA occurs via the thiol-gold bound. In addition, the presence of thiol leads to a denser ssDNA layer adsorbed on GNRs. The smear pattern observed for samples prepared in 1x PBS, 5 mM CTAB is certainly due to the polydispersity of the GNRs stock solution as can be observed in TEM images (Figure S1).

For samples incubated with 300 and 500 nM of SH-D1-Cy3, a contrast signal can be detected at the migration distance where free SH-D1-Cy3 migrates (lane 3), suggesting that the samples are difficult to rinse due to electrostatic interactions. We notice that for GNRs incubated with D1-Cy3, no free DNA can be detected, suggesting that the samples are well rinsed and that no non-specific interactions could be detected. We can suggest that at 300 nM and 500 nM of ssDNA used for the incubation with GNRs, the SH-D1-Cy3 surface density on GNRs is high. The rinsing process of all the unbound ssDNA becomes therefore more difficult. Nevertheless, these non-specific interactions are negligeable compared to the specific interactions, as the contrast of the image demonstrates.

The incubation of GNRs diluted in 0.75 mM CTAB with 20 nM SH-D1-Cy3 allowed the loaded sample to migrate in the gel toward the positive electrode (Figure 5, lane 3). The migration of GNRs in the gel was not influenced by their incubation with higher concentrations of ssDNA (lanes 4, 5, and 6).

https://doi.org/10.1021/acsabm.0c01522
ACS Appl. Bio Mater. XXXX, XXX, XXX−XXX

Measurement of the fluorescence emission of SH-D1-Cy3 in the same gel allowed correlation of the migration of ssDNA with the migration of GNRs (right panel of Figure 5). Lane 2 corresponds to the SH-D1-Cy3 reference; the band detected in the gel after migration corresponds therefore to the migration of free ssDNA.

No signal of SH-D1-Cy3 was detected in the gel for samples of GNRs incubated with increasing concentrations of ssDNA in 0.75 mM CTAB in water (lanes 3, 4, 5, and 6 in the right panel of Figure 5). It is clear that some ssDNA was adsorbed on GNRs since the GNRs migrated in the gel after incubation. The surface density of ssDNA on GNRs in a condition where sequestration was characterized is certainly too low to be detected. Furthermore, at low surface density, ssDNA is oriented toward the surface (lying down) leading to the quenching of the emission of fluorescence.[35]

We conclude that the immobilization efficiency of SH-ssDNA on GNRs in 0.75 mM CTAB in water is much lower than in the condition 1x PBS, 5 mM CTAB. Therefore, the ssDNA sequestration by CTAB prevents from the immobilization of SH-ssDNA on the GNR surface.

CONCLUSIONS

We studied in detail the sequestration effect of CTAB on ssDNA in solution and its influence on the controlled immobilization of thiolated ssDNA on gold nanorods. We used FRET to demonstrate that sequestration could be efficient as it could keep two non-complementary strands together in a compartment or prevent two complementary strands from hybridizing. The condition in which no sequestration was observed (1x PBS, 5 mM CTAB) allowed the control of the immobilization efficiency of thiolated ssDNA on GNRs. Indeed, we demonstrated that the ssDNA surface density depends directly on the ssDNA concentration present in the colloidal solution during immobilization. This observation was confirmed by the fluorescence analysis of gels after electrophoresis of the GNRs functionalized with different densities of ssDNA. In the case of samples prepared in 0.75 mM CTAB where sequestration was taking place, no ssDNA bound to GNRs could be detected which supports the results obtained with FRET on the sequestration effect of DNA by CTAB.

ASSOCIATED CONTENT

Supporting Information

The Supporting Information is available free of charge at https://pubs.acs.org/doi/10.1021/acsabm.0c01522.

Experimental details, TEM images, fluorescent emission intensity and UV-Vis spectroscopy spectrum, and gel electrophoresis (PDF).

AUTHOR INFORMATION

Corresponding Author

Claude Nogues − *Laboratoire de Biologie et Pharmacologie Appliquée, CNRS (UMR 8113), IDA (FR 3242), ENS Paris-Saclay, Université Paris-Saclay, 91190 Gif-sur-Yvette, France;* Present Address: ENS Paris-Saclay, Kimialys SAS, 4 avenue des Sciences, 91190 Gif-sur-Yvette, France.; orcid.org/0000-0002-4189-080X; Email: claude.nogues@ens-paris-saclay.fr

Authors

Henryk J. Łaszewski − *Laboratoire de Biologie et Pharmacologie Appliquée, CNRS (UMR 8113), IDA (FR 3242), ENS Paris-Saclay, Université Paris-Saclay, 91190 Gif-sur-Yvette, France; Université Paris-Saclay, CNRS, ENS Paris-Saclay, CentraleSupélec, LuMIn, 91190 Gif-sur-Yvette, France*

Bruno Palpant − *Université Paris-Saclay, CNRS, ENS Paris-Saclay, CentraleSupélec, LuMIn, 91190 Gif-sur-Yvette, France;* orcid.org/0000-0003-1376-2533

Malcolm Buckle − *Laboratoire de Biologie et Pharmacologie Appliquée, CNRS (UMR 8113), IDA (FR 3242), ENS Paris-Saclay, Université Paris-Saclay, 91190 Gif-sur-Yvette, France*

Complete contact information is available at: https://pubs.acs.org/10.1021/acsabm.0c01522

Author Contributions

The manuscript was written through contributions of all authors. All authors have given approval to the final version of the manuscript.

Funding

H.J.L. acknowledges the funding support from the University of Paris-Saclay through the Initiative Doctorale Interdisciplinaire fellowship.

Notes

The authors declare no competing financial interest.

REFERENCES

(1) Vigderman, L.; Khanal, B. P.; Zubarev, E. R. Functional Gold Nanorods: Synthesis, Self-Assembly, and Sensing Applications. *Adv. Mater.* **2012**, *24* (36), 4811−4841.

(2) Stone, J.; Jackson, S.; Wright, D. Biological Applications of Gold Nanorods. *Wiley Interdiscip. Rev.: Nanomed. Nanobiotechnol.* **2011**, *3* (1), 100−109.

(3) Alkilany, A. M.; Thompson, L. B.; Boulos, S. P.; Sisco, P. N.; Murphy, C. J. Gold Nanorods: Their Potential for Photothermal Therapeutics and Drug Delivery, Tempered by the Complexity of Their Biological Interactions. *Adv. Drug Delivery Rev.* **2012**, *64* (2), 190−199.

(4) Ma, Z.; Xia, H.; Liu, Y.; Liu, B.; Chen, W.; Zhao, Y. Applications of Gold Nanorods in Biomedical Imaging and Related Fields. *Chin. Sci. Bull.* **2013**, *58* (21), 2530−2536.

(5) Zhang, Z.; Wang, J.; Chen, C. Gold Nanorods Based Platforms for Light-Mediated Theranostics. *Theranostics* **2013**, *3* (3), 223−238.

(6) Bradner, J. E.; Hnisz, D.; Young, R. A. Transcriptional Addiction in Cancer. *Cell* **2017**, *168* (4), 629−643.

(7) Le, B. T.; Raguraman, P.; Kosbar, T. R.; Fletcher, S.; Wilton, S. D.; Veedu, R. N. Antisense Oligonucleotides Targeting Angiogenic Factors as Potential Cancer Therapeutics. *Mol. Ther.–Nucleic Acids* **2019**, *14*, 142−157.

(8) Mansoori, B.; Sandoghchian Shotorbani, S.; Baradaran, B. RNA Interference and Its Role in Cancer Therapy. *Adv. Pharm. Bull.* **2014**, *4* (4), 313−321.

(9) Pai, S. I.; Lin, Y.-Y.; Macaes, B.; Meneshian, A.; Hung, C.-F.; Wu, T.-C. Prospects of RNA Interference Therapy for Cancer. *Gene Ther.* **2006**, *13* (6), 464−477.

(10) Kirui, D. K.; Krishnan, S.; Strickland, A. D.; Batt, C. A. PAA-Derived Gold Nanorods for Cellular Targeting and Photothermal Therapy. *Macromol. Biosci.* **2011**, *11* (6), 779−788.

(11) Xie, X.; Liao, J.; Shao, X.; Li, Q.; Lin, Y. The Effect of Shape on Cellular Uptake of Gold Nanoparticles in the Forms of Stars, Rods, and Triangles. *Sci. Rep.* **2017**, *7* (1), 3827.

(12) Sau, T. K.; Murphy, C. J. Seeded High Yield Synthesis of Short Au Nanorods in Aqueous Solution. *Langmuir* **2004**, *20* (15), 6414−6420.
(13) da Silva, J. A.; Netz, P. A.; Meneghetti, M. R. Growth Mechanism of Gold Nanorods: The Effect of Tip-Surface Curvature As Revealed by Molecular Dynamics Simulations. *Langmuir* **2020**, *36* (1), 257−263.
(14) Leonov, A. P.; Zheng, J.; Clogston, J. D.; Stern, S. T.; Patri, A. K.; Wei, A. Detoxification of Gold Nanorods by Treatment with Polystyrenesulfonate. *ACS Nano* **2008**, *2* (12), 2481−2488.
(15) Alkilany, A. M.; Nagaria, P. K.; Hexel, C. R.; Shaw, T. J.; Murphy, C. J.; Wyatt, M. D. Cellular Uptake and Cytotoxicity of Gold Nanorods: Molecular Origin of Cytotoxicity and Surface Effects. *Small* **2009**, *5* (6), 701−708.
(16) Pellas, V.; Hu, D.; Mazouzi, Y.; Mimoun, Y.; Blanchard, J.; Guibert, C.; Salmain, M.; Boujday, S. Gold Nanorods for LSPR Biosensing: Synthesis, Coating by Silica, and Bioanalytical Applications. *Biosensors* **2020**, *10* (10), 146.
(17) Choi, W. I.; Sahu, A.; Kim, Y. H.; Tae, G. Photothermal Cancer Therapy and Imaging Based on Gold Nanorods. *Ann. Biomed. Eng.* **2012**, *40* (2), 534−546.
(18) Tong, L.; Wei, Q.; Wei, A.; Cheng, J.-X. Gold Nanorods as Contrast Agents for Biological Imaging: Optical Properties, Surface Conjugation and Photothermal Effects. *Photochem. Photobiol.* **2009**, *85* (1), 21−32.
(19) Takahashi, H.; Niidome, Y.; Niidome, T.; Kaneko, K.; Kawasaki, H.; Yamada, S. Modification of Gold Nanorods Using Phosphatidylcholine to Reduce Cytotoxicity. *Langmuir* **2006**, *22* (1), 2−5.
(20) Niidome, Y.; Honda, K.; Higashimoto, K.; Kawazumi, H.; Yamada, S.; Nakashima, N.; Sasaki, Y.; Ishida, Y.; Kikuchi, J. Surface Modification of Gold Nanorods with Synthetic Cationic Lipids. *Chem. Commun.* **2007**, No. 36, 3777−3779.
(21) Dai, Q.; Coutts, J.; Zou, J.; Huo, Q. Surface Modification of Gold Nanorods through a Place Exchange Reaction inside an Ionic Exchange Resin. *Chem. Commun.* **2008**, No. 25, 2858−2860.
(22) Niidome, T.; Yamagata, M.; Okamoto, Y.; Akiyama, Y.; Takahashi, H.; Kawano, T.; Katayama, Y.; Niidome, Y. PEG-Modified Gold Nanorods with a Stealth Character for in Vivo Applications. *J. Controlled Release* **2006**, *114* (3), 343−347.
(23) Wang, C.-H.; Chang, C.-W.; Peng, C.-A. Gold Nanorod Stabilized by Thiolated Chitosan as Photothermal Absorber for Cancer Cell Treatment. *J. Nanopart. Res.* **2011**, *13* (7), 2749−2758.
(24) Thierry, B.; Ng, J.; Krieg, T.; Griesser, H. J. A Robust Procedure for the Functionalization of Gold Nanorods and Noble Metal Nanoparticles. *Chem. Commun.* **2009**, No. 13, 1724−1726.
(25) Paul, B. K.; Guchhait, N. Exploring the Strength, Mode, Dynamics, and Kinetics of Binding Interaction of a Cationic Biological Photosensitizer with DNA: Implication on Dissociation of the Drug-DNA Complex via Detergent Sequestration. *J. Phys. Chem. B* **2011**, *115* (41), 11938−11949.
(26) Neugebauer, J. M. [18] Detergents: An Overview. In *Methods in Enzymology*; Elsevier: New York, 1990; Vol. *182*, pp 239−253 DOI: 10.1016/0076-6879(90)82020-3.
(27) Dias, R. S.; Lindman, B.; Miguel, M. G. DNA Interaction with Catanionic Vesicles. *J. Phys. Chem. B* **2002**, *106* (48), 12600−12607.
(28) Orendorff, C. J.; Murphy, C. J. Quantitation of Metal Content in the Silver-Assisted Growth of Gold Nanorods. *J. Phys. Chem. B* **2006**, *110* (9), 3990−3994.
(29) Santhiya, D.; Maiti, S. An Investigation on Interaction between 14mer DNA Oligonucleotide and CTAB by Fluorescence and Fluorescence Resonance Energy Transfer Studies. *J. Phys. Chem. B* **2010**, *114* (22), 7602−7608.
(30) Techen, A.; Hille, C.; Dosche, C.; Kumke, M. U. Fluorescence Study of Drug-Carrier Interactions in CTAB/PBS Buffer Model Systems. *J. Colloid Interface Sci.* **2012**, *377* (1), 251−261.
(31) Oh, T.; Takahashi, T.; Kim, S.; Heller, M. J. CTAB Enhancement of FRET in DNA Structures. *J. Biophotonics* **2016**, *9* (1−2), 49−54.
(32) Sikorska, E.; Wyrzykowski, D.; Szutkowski, K.; Greber, K.; Lubecka, E. A.; Zhukov, I. Thermodynamics, Size, and Dynamics of Zwitterionic Dodecylphosphocholine and Anionic Sodium Dodecyl Sulfate Mixed Micelles. *J. Therm. Anal. Calorim.* **2016**, *123* (1), 511−523.
(33) Naskar, B.; Dey, A.; Moulik, S. Counter-Ion Effect on Micellization of Ionic Surfactants: A Comprehensive Understanding with Two Representatives, Sodium Dodecyl Sulfate (SDS) and Dodecyltrimethylammonium Bromide (DTAB). *J. Surfactants Deterg.* **2013**, *16* (5), 785−794.
(34) Demers, L. M.; Mirkin, C. A.; Mucic, R. C.; Reynolds, R. A.; Letsinger, R. L.; Elghanian, R.; Viswanadham, G. A Fluorescence-Based Method for Determining the Surface Coverage and Hybridization Efficiency of Thiol-Capped Oligonucleotides Bound to Gold Thin Films and Nanoparticles. *Anal. Chem.* **2000**, *72* (22), 5535−5541.
(35) Schneider, G.; Decher, G.; Nerambourg, N.; Praho, R.; Werts, M. H. V.; Blanchard-Desce, M. Distance-Dependent Fluorescence Quenching on Gold Nanoparticles Ensheathed with Layer-by-Layer Assembled Polyelectrolytes. *Nano Lett.* **2006**, *6* (3), 530−536.

https://doi.org/10.1021/acsabm.0c01522
ACS Appl. Bio Mater. XXXX, XXX, XXX−XXX